MScMS-II: an innovative IR-based indoor coordinate measuring system for large-scale metrology applications

MScMS-II: an innovative IR-based indoor coordinate measuring system for large-scale metrology applications

Maurizio Galetto · Luca Mastrogiacomo · Barbara Pralio

Abstract According to the current great interest concerning large-scale metrology applications in many different fields of manufacturing industry, technologies and techniques for dimensional measurement have recently shown a substantial improvement. Ease-of-use, logistic and economic issues, as well as metrological performance are assuming a more and more important role among system requirements. This paper describes the architecture and the working principles of a novel infrared (IR) optical-based system, designed to perform low-cost and easy indoor coordinate measurements of large-size objects. The system consists of a distributed network-based layout, whose modularity allows fitting differently sized and shaped working volumes by adequately increasing the number of sensing units. Differently from existing spatially distributed metrological instruments, the remote sensor devices are intended to provide embedded data elaboration capabilities, in order to share the overall computational load. The overall system functionalities, including distributed layout configuration, network self-calibration, 3D point localization, and measurement data elaboration, are discussed. A preliminary metrological characterization of system performance, based on experimental testing, is also presented.

Keywords Large-scale metrology · Distributed measurement systems · Wireless sensor networks · Indoor dimensional measurement · Infrared-based tracking

M. Galetto (✉) · L. Mastrogiacomo · B. Pralio
Politecnico di Torino, Dipartimento di Sistemi di Produzione ed Economia dell'Azienda,
Corso Duca degli Abruzzi 24,
10129 Turin, Italy
e-mail: maurizio.galetto@polito.it

1 Introduction

The field of large-scale metrology (LSM) applies to angular measurement and alignment techniques as well as length measurement of large machines and structures, whose linear dimensions range from tens to hundreds of meters. Since its definition in the late 1970s, this field has been considered as "one which provides a significant challenge to the metrologist since virtually every project is different and, moreover, accuracy requirements are becoming more demanding" [30]. The attention of manufacturers has been focused on the more and more demanding accuracy requirements. As a matter of fact, many different industrial sectors, such as aerospace, automotive, shipbuilding, and railway, demonstrate a great interest in large-scale metrology applications. Reliable and efficient metrological instruments are needed to provide a support in assembly, alignment, measurement inspection, and robot tracking tasks.

Due to the needs for measuring medium and large-sized objects, generally unhandy and difficult to move, the classical coordinate measuring machine (CMM)-like approach is revised, and the metrological instrument is moved to the object to be measured and adequately arranged within the available working volume. As required, accuracy standards strongly affect their economic impact; most of these systems may not be cost-effective for measurements below a given level of accuracy. According to this, novel systems should found their competitiveness on logistic as well as economic issues, besides than system performance.

A basic list of requirements of a LSM system should include [11]:

– Portability: it is intended as the capability of the system to be easily moved within the working environment;

- Flexibility: it refers to system capabilities to apply to different working environments and to perform various measurement tasks;
- Handiness: it means easiness of installation and use;
- Scalability: it refers to the capability to cover differently sized and shaped volumes;
- Metrological performance: it encounters for measurement characterization, in terms of stability, repeatability, reproducibility, and accuracy;
- Economic impact: it takes into account, besides the product price, the maintenance costs and the training costs.

Several solutions based on different technologies have been proposed for metrology systems, based on optical, mechanical, electromagnetic, inertial, and acoustic technologies. At present, optical-based systems clearly demonstrate their advantages over the other approaches and their potentialities for large-scale metrology applications. As noted by Estler in 2002 [7], tremendous improvements have been achieved in this field due to advancements in optical technology and fast, low-cost computation. However, it is recognized that significant technical challenges still remain "associated with high accuracy measurements of large structures". A recent state-of-the-art update [29] discusses further developments in the field, in terms of new techniques for improving system flexibility, internationally recognized standards for evaluating performance, and bridge designs for adequately responding to the needs of manufacturers. A few optical-based techniques compete for LSM applications, ranging from theodolites, total stations, digital photogrammetry to the more recent laser trackers, optical scanners, and indoor global positioning system (GPS). According to these methods, several systems have been designed, aimed at exhaustively matching performance as well as practical requirements.

Different classifications can be proposed for these instruments, based on the working principles, the measurement operating conditions, or the sensor layout.

According to optical-based systems, working principles refer to two angles and one length (laser tracker, laser radar, and total stations), multiple angles (camera-based triangulation, indoor GPS, and photogrammetry), or multiple lengths (multiple laser trackers) [6]. Furthermore, the measurement operating conditions give rise to a classification between contact and non-contact instruments. The former category includes target-based systems, following reflective targets positioned against the object to be measured, and probe-based systems, tracking the position of measuring probes directly touching the object. On the other hand, due to the pressing need for portable, flexible, and scalable systems, the attention have been recently focused on novel approaches to the sensor displacement. As a consequence, distributed systems, consisting of multiple units spread out over the working environment, represent a novel alternative to the classical centralized approach, founding on a stand-alone independent measuring unit.

This paper presents a novel optical-based distributed system [Mobile Spatial coordinate Measuring System-II (MScMS-II)], designed to perform low-cost, simple, and rapid indoor coordinate measurements of large-sized objects. The novelty of the system is mainly related to its capabilities to extend the measurement domain, being able to cover large and geometrically complex working volumes by properly distributing the network sensors, and to consistently reduce the economic impact.

Several optical-based systems are industrially available, providing well-settled solutions to the needs for accurate and reliable measuring instruments for indoor large-scale metrology applications. The design phase of such systems has been strongly influenced by the requirements for a portable and flexible system, able to fit more and more different application scenarios. These requirements are addressed by many manufacturers through the integration of six DoF probes, able to perform a variety of measurement tasks (such as reconstruction of geometrical features, object shape definition, and shape changes monitoring) as well as to deal with hardly accessible features.

Laser tracker-based systems are available from many manufacturers ([2, 3, 8, 19]) and are the more common and conventional response to the need for a flexible, portable, and highly accurate alternative to CMMs. More recent designs are based on laser tracking and photogrammetry, by integrating a camera into the laser tracker to measure the 6DoF pose of a mobile contact probe [19]. Other hybrid systems combine laser tracker, cameras, and tilting sensors to estimate the probe pose, entrusting range measurements to the laser tracker and angular measurements to the camera-based sensor set [2, 3].

Theodolites and total stations [20], commonly used in surveying and engineering work, are a portable, easy to use, and cheaper alternatives to laser trackers, but they provide lower accuracy and appear to be unsuitable to measure complex shapes.

Pure digital photogrammetry-based systems gather images either with a single moving camera (offline photogrammetry) or with a set of synchronized cameras (online stereo/multi-image photogrammetry) [22]. Advanced online camera-based systems, such as ([4, 24, 26–28]), provide capabilities to perform different measurement task, possibly combined with targeted handheld probes. These systems, mounting cameras in a fixed bar housing, implement a centralized approach to solve the sensor displacement problem and hence reduce their scalability properties. System accuracy is strongly related to image quality (related to the hardware resolution), 3D point reconstruction algorithms (bundle adjustment), and working

environment conditions (lighting effects generating reflections).

The innovative indoor-GPS ([1, 26]), performing triangulation of rotating laser beams emitted by multiple transmitters (reference points), represents a highly accurate metrological solution. It provides distinguishing flexibility and portability features due to its network-based architecture combined with a mobile measuring probe.

All these systems, sharing significant capabilities to fulfill design requirements, have also a high economic impact, mainly related to the sensing hardware.

The proposed IR-based system (MScMS-II), which shares the digital photogrammetry principles with the novel camera-based solutions [25], demonstrates to better face with scalability issues, due to its distributed and modular architecture. Although this system appears to have lower economic impact charged to worse metrological performance, it is noteworthy that these aspects are strongly related to the technical specifications of sensing devices (e.g., camera resolution, sample rate, and light emitting diode (LED) intensity). On the other hand, further improvement could be obtained by integrating the proposed system with other accurate optical-based systems (e.g., instruments using structured light). Such a multi-resolution integrated solution should be able to exploit the high performance of these centralized systems within the large working volume covered by the distributed sensor network.

In Table 1, the MScMS-II is compared with existing solutions, focusing on its capabilities to address the basic requirements of an LSM instrument. It has to be noted that the economic impact, which is reported in the last column of Table 1, has been referred to the purchasing cost only.

The paper is organized as follows. In section 2, the system architecture, the working principles of the basic units and their hardware/software relationships are outlined. Working principles are further described in section 3 and section 4, where localization schemes and system calibration are faced through algorithmic implementation. The system is, then, characterized by a set of experimental tests. The preliminary results, reported in section 5, aim at evaluating measurement stability, repeatability, reproducibility, and accuracy. Finally, section 6 reports some concluding remarks and a brief outline of future research.

2 System description

The MScMS-II is an indoor coordinate measuring system based on IR optical technology, designed for large-scale metrology applications. The system, developed at the Industrial Metrology and Quality Engineering Laboratory of DISPEA–Politecnico di Torino, consists of three basic units (Fig. 1): a network ("constellation") of wireless sensor devices, suitably distributed within the measurement volume, to estimate 3D coordinates of reflective passive markers; a mobile wireless and armless probe, equipped with two reflective markers, to "touch" the measurement points, providing capabilities to walk around the object to be measured without being bounded by a mechanical arm; a data processing system, using Bluetooth connection, to acquire and elaborate data sent by each network node.

A first prototype of the MScMS had been implemented, exploiting ultrasound (US) transceivers to communicate and evaluate mutual distances between the distributed sensor nodes and the handheld probe [11]. The previous US-based system and the herein presented IR-based system share the distributed system architecture, as well as issues related to the beacon positioning problem [13, 14], the measurement task procedure [11], and the testing practices for evaluating system performance [10]. On the other hand, the two systems are based on different calibration procedures and implement different localization algorithms (triangulation for

Table 1 Qualitative comparison of optical-based distributed systems for large-scale metrology

System	Requirements					
	Portability	Flexibility	Handiness	Scalability	Metrological performance	Purchasing cost [k€]
Laser tracker	Medium	Medium	Medium	Low	High	80 - 150
Laser radar	Medium	Medium	Medium	Low	High	400 - 500
Digital photogrammetry	High	Medium	High	Medium	High	20 - 100
Indoor GPS	High	High	Medium	High	High	>150[(a)]
Theodolite/total station	High	Low	High	High/medium	Low	1–4
MScMS-II	High	High	High	High	Medium	>3[a]

The last column reports a rough estimation of the economic impact (referred to the purchasing cost), expressed in k€. The wide range of variation of costs is related to the fact that different manufacturers offer metrology instruments with different performance levels and accessories

[a] It has to be noted that the economic impact of the two distributed systems (indoor GPS and MScMS-II) is strongly related to the network sizing, i.e., the number of remote sensor devices. The reported values refer to the minimum number of sensors needed to perform network calibration (i.e., three sensing units)

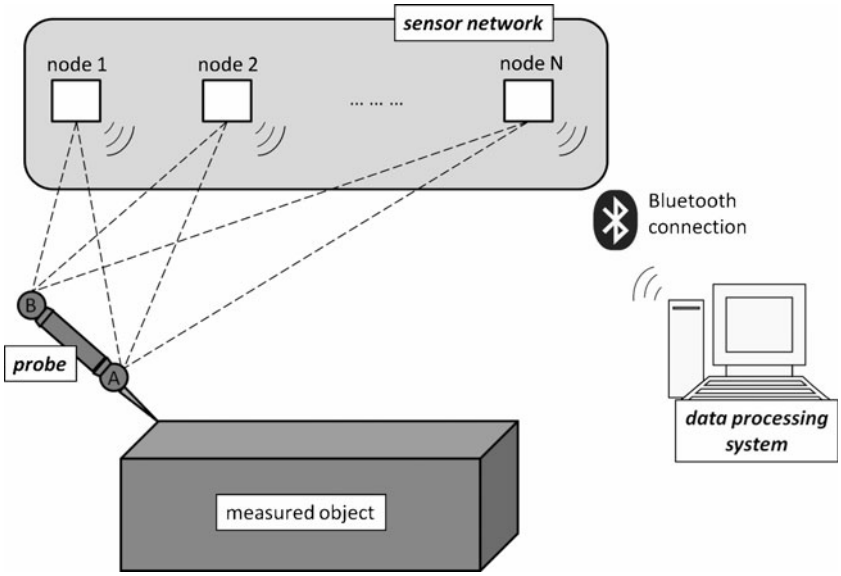

Fig. 1 MScMS-II architecture. The *dashed lines* represent visual links between sensor nodes and retro-reflective spheres (indicated as *A* and *B*) equipping the handheld probe. The Bluetooth connection is established between each node and the processing system

the IR-based MScMS and trilateration for the US-based MScMS). The MScMS-II has been designed and developed to represent an improvement as to functional, logistic, economic, and metrological issues. From a functional point of view, the sampling rate, which has been increased from two points per second for the US-based system to up to 100 points per second for the MScMS-II, allows to dynamically tracking moving objects and, hence, to enhance measurement automation potentialities [15]. The use of lightweight passive reflective markers instead of energy-consuming US sensing devices allows more flexibility as to probe design and sensor carrying solutions. Furthermore, due to the size and geometry of the field-of-sensing and the minimum sensor data required for triangulation, the beacon density for 3D point localization is consistently reduced in the MScMS-II. This issue entails an improvement as to installation times and overall cost. The higher level of automation and metrological effectiveness, which characterize the calibration procedure of the MScMS-II, represent a further point for the IR-based system, reducing setup times and human skills requirements. Whereas some critical features of US devices (non-punctiform dimensions, speed of sound dependence on operating temperature, wave reflection, and diffraction, etc.) caused a low accuracy in the measurement results [11, 12], the MScMS-II provides a consistent improvement of metrological performance, by increasing position accuracy and measurement reliability.

2.1 Sensor network

Currently, a prototype of the distributed network has been set up by using commercial low-cost IR cameras, characterized by an interpolated resolution of 1024×768 pixels (native resolution is 128×96 pixels), a maximum sample rate of 100 Hz, and a field of view (FOV) of approximately 45°×30°. Each camera implements a real-time multi-object tracking engine, which allows tracking up to four IR light sources. In order to work with passive markers, each camera was coupled with a near-IR light source (Fig. 2), consisting of a 160-chip LED array with a peak wavelength of 940 nm and a viewing half-angle of approximately 80°. The overall sensor set (camera and LED array) weights about 500 g and is sized 13×13×15 cm. The IR sensor configuration can be set according to shape and size of the measured object as well as of the working environment [15]. Fig. 3 provides a virtual reconstruction of the working layout, with reference to a six-camera configuration.

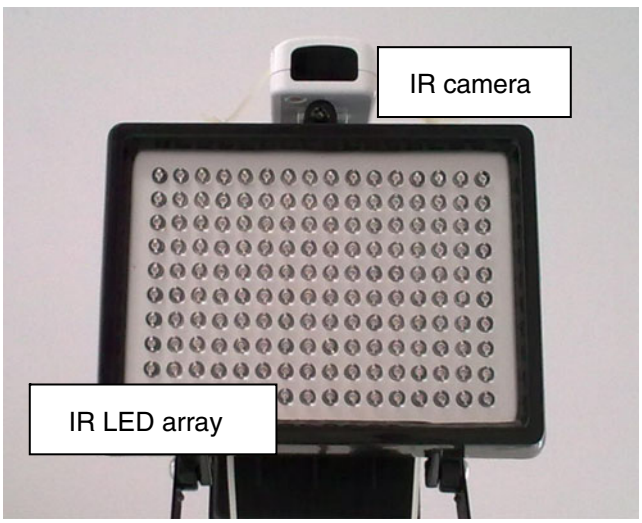

Fig. 2 Main components of the IR-based sensor network: an IR camera is coupled with an IR LED array to locate passive retro-reflective targets

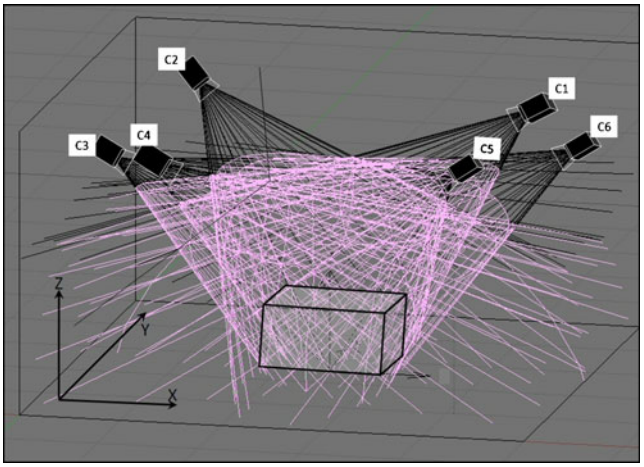

Fig. 3 Virtual reconstruction of the working layout. The *black wireframe* represents the camera "field-of-sensing", whereas the *light gray wireframe* represents the working volume (interpreted as the volume of intersection of at least two "field-of-sensing"). A 1.5 m× 0.8 m×0.5 m *box*, representing a reference object to be measured, has been placed within the working environment

Given a fixed number of cameras, all operating conditions being unchanged, the actual working volume, intended as the region within which the spatial position of a single marker can be reconstructed, depends on the technical specifications of IR cameras (e.g., FOV, sensitivity, pixel resolution, and focal length) and light sources (e.g., LED power and wave length) as well as on the size of the markers. According to triangulation principles, this volume consists of the volume of intersection of the "field-of-sensing" of at least two cameras. It has to be noted that a network layout consisting of six commercial low-cost IR sensors, arranged in a 5.0× 6.0×3.0 m working environment according to a grid-based configuration, results in an actual working volume of about 2.0×2.0×2.0 m.

2.2 Measuring probe

The mobile probe (Fig. 4) consists of a rod, equipped with two reflective markers at the extremes and a stick at one end to physically "touch" the measurement points. Passive markers have been made by wrapping around polystyrene spheres a retro-reflective silver transfer film. The marker dimensions depend on hardware capabilities and working volume. The IR sensor sensitivity has been experimentally evaluated by testing visibility distance of differently sized retro-reflective spheres. The implemented technology demonstrated to be able to track a 40-mm diameter marker at a maximum distance of 6 m. It is noteworthy that, due to its lightweight and simple design, the measuring probe could be handheld as well as carried onboard by an autonomous agent (ground or aerial robot), providing up to 6DoF in performing the measurement task.

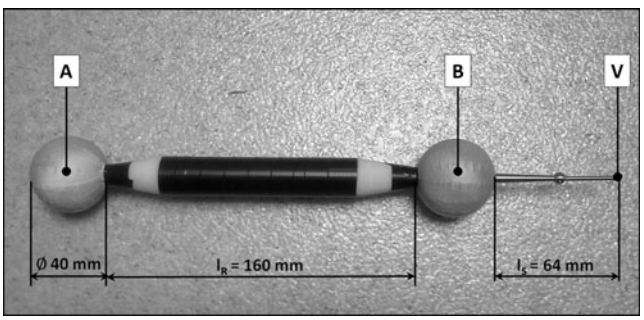

Fig. 4 Mobile measuring probe

Referring to Fig. 4, as the probe tip (V) lies on the same line of the centers of the markers (A, B), spatial coordinates of point $X_V \equiv (x_V, y_V, z_V)$ can be univocally determined by the following linear equation:

$$\mathrm{X}_V = \mathrm{X}_A + \frac{(\mathrm{X}_B - \mathrm{X}_A)}{\|\mathrm{X}_B - \mathrm{X}_A\|} \cdot \mathrm{d}_{V-A} \tag{1}$$

where $X_A \equiv (x_A, y_A, z_A)$ and $X_B \equiv (x_B, y_B, z_B)$ identify the centers of marker A and B, respectively. The term

$$\mathrm{d}_{V-A} = \|\mathrm{X}_V - \mathrm{X}_A\| \tag{2}$$

is a priori known as it depends on probe geometry.

2.3 Data processing system

The data processing hardware consists of a 2.5 GHz computer platform, connected to a set of IR cameras via a Bluetooth link. Each camera provides for the data processing system the 2D coordinates of the IR spot(s) in its view plane. As a matter of fact, the embedded real-time tracking capabilities of the IR sensor save the computational effort for performing the image analysis and spot coordinates identification by the computer platform. As the connection is based on a Bluetooth link, cameras are sequentially sampled. Hence, image synchronization represents a critical issue for 3D reconstruction performance, depending on acquisition delays. According to the hardware–software configuration, a maximum number of six IR sensors can be managed by a single PC unit. A modular approach, based on multiple processing units sharing the information of different camera sets, can be implemented to enlarge the working volumes. Considering that the probe is steadied during measurement, with a configuration of six non-synchronized cameras, and using a sampling rate of 50 Hz, preliminary tests showed that the acquisition delay has a negligible influence on measurement results. On the other hand, given that synchronization could represent a criticality for tracking dynamic objects, this issue will be delved into in future research.

The processing software implements layout evaluation, system calibration, 3D point localization, and data elaboration procedures. The layout evaluation block, according to the working environment description and the measurement task characterization, provides a graphical interpretation of different configuration solutions, i.e., sensor spatial distributions within the available volume. This "pre-processing" tool provides for computing and drawing the coverage volume, i.e., the volume covered by at least n cameras. Furthermore, it could perform as an offline diagnostic tool, reporting operating conditions that could give rise to possible ambiguities in 2D–3D reconstruction. The analyzed configurations can be either user-defined or algorithm-assisted. A computer-assisted procedure for optimal sensor placement can be used to configure the network layout in order to optimize the system performance [14].

According to a given network configuration, the calibration block implements a camera self-localization algorithm. Taking as input from the camera tracking engine the 2D position estimates of a single reflective marker (calibration marker), randomly moved in several unknown positions within the working volume, it provides camera positions and orientations as well as camera internal parameters (such as focal length and lens distortion). Locating a calibrated artifact (calibration square) positioned within the working volume, it performs camera alignment and scaling to a user-defined coordinate reference system.

These information are then used by the localization algorithm to perform 3D reconstruction of measurement points, according to digital photogrammetry principles [25]. The data elaboration software tool has been designed as to accomplish system flexibility, by providing capabilities to perform single-point coordinate measurements, distance measurements, as well as geometry reconstruction. To this end, functions similar to those implemented by CMM commercial packages have been integrated to support the user in elaborating the measurement data and reconstructing basic geometric features [18].

3 Localization algorithm

Given a camera layout (i.e., n_c cameras, with known technical characteristics, positions, and orientations) focused on m markers, for each m-uple of 2D pixel coordinates $u_{ij} \equiv (u_{ij}, v_{ij})$, with $i = 1,\ldots,n_c$ and $j = 1,\ldots,m$, the localization algorithm provides the 3D coordinates of the corresponding m retro-reflective markers (Fig. 5).

The localization procedure, following the fundamentals of digital photogrammetry, is articulated in two main steps:

1. Find the correspondences among pixels in different image views
2. Match the 2D information of different camera views for recovering the spatial coordinates of the 3D point

As to the first step, it consists in reconstructing the matrix M of 2D pixel coordinates corresponding to the projection of the same 3D point onto the camera image planes. Since a generic marker j, positioned at unknown 3D coordinates X_{Mj}, might not be visible from all the cameras (e.g., out of the field of vision, shadowed), $M \in \mathbb{R}^{p \times 2}$ where $p \leq n$.

Epipolar geometry, i.e., the intrinsic projective geometry between two views, has been used to correlate information from multiple camera images [16, 21]. The correlation between two 2D pixels, $U(u,v)$ and $U'(u',v')$, detected by two different cameras, states to what extent they can be considered as the projections of the same 3D point onto the camera image planes. According to epipolar geometry principles, given a pair of images, to a generic point U in the first image corresponds a line ℓ (i.e., the epipolar line) in the second image (see Fig. 6). The epipolar line is defined as the intersection of the image plane of the second camera with the plane passing through the point U and the two camera centers, X_{C1} and X_{C2}, which will also contain the reconstructed 3D point X_M. This line can be drawn whenever the projection matrices of the given pair of cameras are known. The image view of the 3D point in the second image U' will thus lie on the epipolar line ℓ. As a matter of fact, the point correspondence can be found by evaluating the distance between the 2D pixel U' in the second image and the epipolar line corresponding to the 2D pixel U in the first image.

As the epipolar distance is proportional to the reprojection error after triangulation, large epipolar distances mean pixel correlation mismatches and large reprojection errors. A threshold method has been implemented to find correspondences between different image views.

The concurrent presence of more than one retro-reflective marker within the working volume could give rise to some ambiguities in measurement point recovery. In some practical cases, probe positioning with respect to the IR sensor and its orientation could correspond to a very small distance between the two pixels in an image view. In order to reduce the errors in pixel correlation, a minimum search approach has been implemented. Stated that two pixels U' and $\mathcal{U}$ in the second camera view verified the threshold constraint, the point U in the first camera view will be correlated to the one having the minimum distance to its epipolar line ℓ.

The second step of the localization algorithm deals with the triangulation problem [17]. Given its 2D positions in n different image planes (with $2 \leq n \leq n_c$), the 3D coordinates of a point X_m can be obtained by intersecting the camera projection lines (triangulation). Hence, the set of $2 \times n$

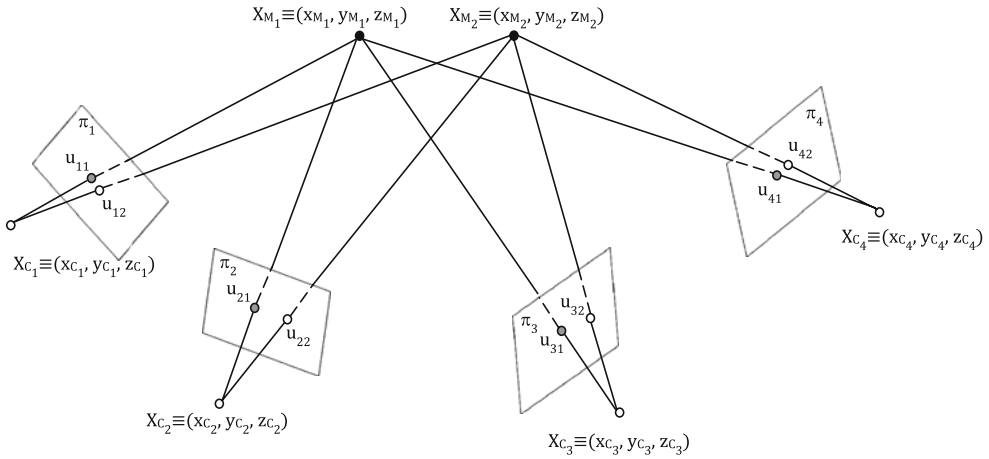

Fig. 5 Graphical representation of the localization problem when a setup of four cameras (n_c=4) is used to reconstruct the 3D position of two markers (m=2). X_{Ci} (with i=1, …, 4) and X_{Mj} (with j=1,2) refer to the 3D coordinates of the ith camera center and the jth marker, respectively. Point u_{ij} represents the 2D projection of X_{Mj} onto the image plane of the ith camera. It corresponds to the intersection of the camera view plane π_i with the projection line of X_{Mj} (i.e., the line passing through the 3D point and the camera center)

equations with unknown variables (x_M, y_M, z_M) can be written as:

$$AX_M - B = 0 \tag{3}$$

where $A \in \mathbb{R}^{2n\times 3}$ and $B \in \mathbb{R}^{2n\times 1}$ are known matrices, whose elements are obtained as functions of camera projection matrices and 2D pixel spatial coordinates $U_i(u,v)$ (with i= 1,…, n).

In practical applications, due to measurement noise and sensor hardware limits, the projection lines do not generally meet in a unique point, and a least-squares minimization is needed using two or more cameras. To this end, a single value decomposition method has been chosen to solve Eq. 3 for X_m, obtaining an approximated vector of position coordinates X_M^*.

According to the vector of residuals $E = \left(AX_M^* - B\right)$, a parameter e, directly proportional to the overall variance, is estimated as [12]:

$$e \propto E^T E \tag{4}$$

This parameter is used as preliminary diagnostics in order to evaluate the correctness of 3D positioning. The estimated coordinates $X_M^*\left(x_M^*, y_M^*, z_M^*\right)$ of the measured point, if characterized by high variance values, are automatically discarded according to a threshold method.

It has to be noted that, as they are based on the 2D image views of different cameras, the triangulation results are strongly affected by camera synchronization issues. As a matter of fact, the 3D point reconstruction algorithm should use the 2D position coordinates of the same point as seen by the different camera sensors at the same time instant (synchronized camera sampling). Whenever a sequential sampling procedure is implemented, the higher is the number of sensors the higher is the total acquisition delay and thus possible discrepancies among different image views. Whereas it could represent a problem for tracking dynamic objects, sequential sampling has negligible influence on measurement performance as data acquisition is made by keeping the probe in static conditions.

4 System calibration

The multi-camera calibration problem is faced by using a fully automatic single-point self-calibration technique ([5, 31]).

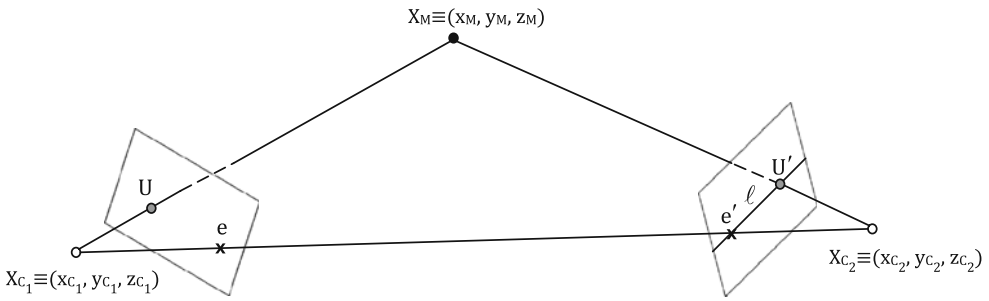

Fig. 6 Epipolar geometry principles [16]. X_{C1} and X_{C2} are the camera centers, X_M is the 3D point. U and U' represent the 2D projection of X_M onto the image planes of the first and second camera, respectively. e and e' are the epipoles of the two cameras, i.e., the intersection of the line joining the two camera centers with the image plane. l is the epipolar line corresponding to point U

Differently from other existing calibration methods [32, 34], the one herein applied does not require positioning a 3D calibration object at known 3D coordinates and is able to reconstruct internal parameters besides positions and orientations of a camera set. Notwithstanding, this extremely flexible, fast, and easy-to-use technique requires a minimum of three cameras as the internal parameters are the same for all cameras, but they are completely unknown. The reference system alignment and scaling procedures are carried out by positioning a calibrated artifact within the working volume. The reference system origin and orientation are thus fixed according to the measurement task and/or the measured object.

According to the calibration procedure, a single reflective marker is randomly moved in several unknown positions within the working volume and tracked by the IR camera sensors. Image acquisition and processing are managed by the camera onboard hardware that directly provides pixel coordinates in the view plane. Modifications to the original MATLAB calibration toolbox in ([5]) have been made to provide as input pixel coordinates instead of pixel images. As a matter of fact, the camera onboard tracking capabilities save the automatic spot detection procedure, which is a computationally expensive operation. On the other hand, camera self-calibration as well as probe localization is affected by the reliability of the embedded tracking engine, i.e., by its capabilities to correctly identify the bright spot in the image and to calculate its position in the camera view.

Firstly, the calibration algorithm performs a two-step procedure for discarding outliers, either due to reflections in the working environment or measurement errors of the tracking engine. False points are removed from the list of visible points of the IR cameras according to an iterative pair-wise analysis and a 2D reprojection error-based strategy. As to the former step, image pairs are iteratively selected according to the number of visible corresponding points. Point-to-point correspondence is analyzed according to epipolar geometry constraints [16, 21] and applying a RANSAC-based technique [9] for discarding outliers. Survived points are further evaluated by projecting them back to the camera pairs and applying a threshold method based on 2D reprojection errors for removing false ones. Then the calibration algorithm implements an iterative procedure that compute the projective structure (i.e., the projection matrix and the cloud of reconstructed 3D points) until outliers are completely removed and estimate a nonlinear distortion model of the camera lens until a stopping condition (either based on a user-defined threshold or a maximum number of iterations) is reached. Finally, this procedure yields five internal camera parameters (focal length, principal point coordinates, skew coefficient, and radial and tangential distortion coefficients) and six external camera parameters (3D position coordinates of the camera center and orientation angles of its optical axis). As the external camera parameters are provided in an unknown reference frame, having the origin in the center of the cloud of points, a further step for aligning and scaling the world coordinate system is needed. To this end, a laser cut aluminum square (300×400 mm sized), measured to submillimeter accuracy by a CMM, is used as calibrated artifact (see Fig. 7a).

5 Preliminary tests

A set of preliminary tests has been carried out to investigate the performance of the overall system, including the distributed sensor network, the handheld measuring probe, and the data processing system. It is noteworthy that the experimental results are strongly related to the network configuration, in terms of number of IR cameras, positioning, and orientation. Data discussed hereafter have been obtained by using a set of six IR cameras, arranged in a working environment similar to the one shown in Fig. 3. The resulting measurement volume was about 2.0×2.0×2.0 m wide. A sampling frequency of 50 Hz has been used for data acquisition.

The system has been evaluated through stability, repeatability, and reproducibility tests and characterized by a preliminary estimation of the measurement accuracy.

The system stability, i.e., the property of a measuring instrument, whereby its metrological properties remain constant in time [33], has been evaluated in $s=15$ different positions, distributed all over the measurement volume. For each position the mobile probe has been kept in a stationary condition, replicating the measurement $k=30$ times, over a span of time of approximately 300 s. Results, which are shown in Table 2, are reported in terms of sample mean and standard deviation of the reconstructed 3D positions of the probe tip V, referring to a user-defined room-aligned reference coordinate system. It is noteworthy that the experimental data are related to the IR system stability in measuring a single point, as well as to the operator skills. As a matter of fact, human skills represent an external factor, related to capabilities in holding the probe in a fixed position during data acquisition.

Repeatability, i.e., "closeness of the agreement between the results of successive measurements of the same measurand carried out under the same conditions of measurement" [33], has been tested on $s=5$ different points, uniformly distributed within the measurement volume. The test has been carried out by repeating the measurement $k=30$ times for each point, repositioning the probe in the same position for each measurement. Results of repeatability tests are reported in Table 3, in

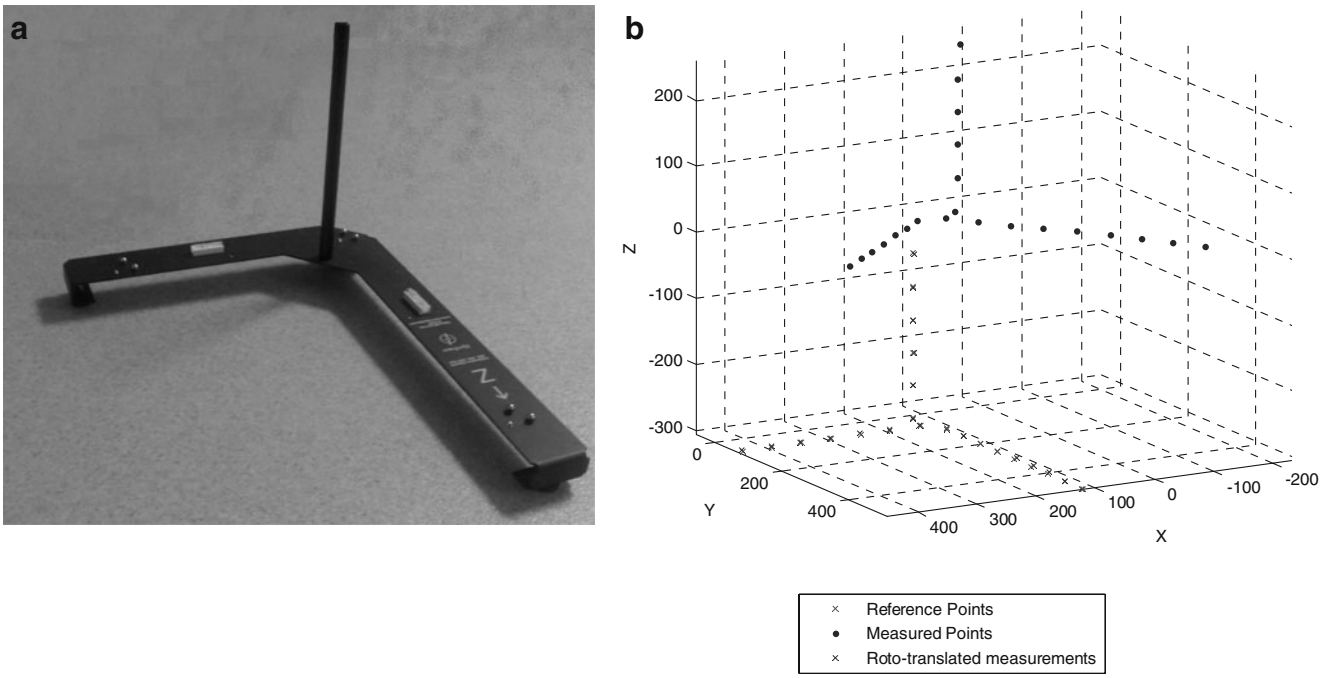

Fig. 7 **a** Reference calibrated artifact—**b** Set up for evaluating the overall system accuracy. The *dots* represent measured points in different positions within the working volume whereas the *crosses* represent the effects of roto-translation based on a RLS fitting approach

terms of sample mean and standard deviation of the reconstructed 3D positions of the probe tip V.

Further performance degradation in terms of standard deviation is strongly related to capabilities of the human operator of exactly replicating the probe position at each test.

Measurement reproducibility, intended as "closeness of the agreement between the results of successive measurements of the same measurand carried out under changed conditions of measurement" [33], has been tested with reference to $s=5$ points, distributed all over the measurement volume. For each point, the measurements have been repeated $k=30$ times with different angular orientations of the mobile probe. Table 4 reports statistical results of these preliminary tests. As expected, the standard deviation is basically higher for reproducibility tests. This behavior can be basically ascribed to the strong influence the relative position and orientation of probe and network devices has on the overall measurement accuracy.

Table 2 Mean and standard deviation results for stability preliminary tests

	$\bar{x}$ [mm]	$\bar{y}$ [mm]	$\bar{z}$ [mm]	$\hat{\sigma}_X$ [mm]	$\hat{\sigma}_Y$ [mm]	$\hat{\sigma}_Z$ [mm]
Point 1	−207.20	−300.35	−83.98	0.18	0.16	0.18
Point 2	−146.96	163.49	−75.87	0.33	0.18	0.22
Point 3	65.29	−40.32	−77.23	0.15	0.28	0.34
Point 4	330.53	329.98	−72.17	0.27	0.24	0.30
Point 5	330.31	−357.60	−74.51	0.14	0.10	0.21
Point 6	257.63	228.29	391.59	0.12	0.31	0.15
Point 7	249.58	−277.87	383.17	0.11	0.17	0.08
Point 8	−193.08	−304.65	392.24	0.39	0.28	0.32
Point 9	−232.05	193.58	397.85	0.15	0.10	0.20
Point 10	15.80	15.20	386.91	0.16	0.09	0.17
Point 11	−221.98	138.48	529.86	0.25	0.13	0.11
Point 12	−172.10	−288.12	520.14	0.29	0.15	0.35
Point 13	0.77	−36.05	514.68	0.14	0.14	0.13
Point 14	250.14	139.75	523.14	0.15	0.15	0.13
Point 15	85.84	−45.91	514.43	0.29	0.38	0.23

The sample mean values refer to a user-defined room-aligned reference coordinate system

Table 3 Mean and standard deviation results for repeatability preliminary tests

	$\bar{x}$ [mm]	$\bar{y}$ [mm]	$\bar{z}$ [mm]	$\hat{\sigma}_X$ [mm]	$\hat{\sigma}_Y$ [mm]	$\hat{\sigma}_Z$ [mm]
Point 1	−179.56	−188.55	−41.99	1.25	0.75	0.69
Point 2	257.70	135.87	−28.46	0.79	0.61	0.36
Point 3	−159.09	182.61	−36.57	0.45	0.43	0.39
Point 4	171.66	−238.84	−29.08	0.61	0.89	0.55
Point 5	−13.92	−23.52	−35.56	0.31	0.34	0.27

The sample mean values refer to a user-defined room-aligned reference coordinate system

A preliminary evaluation of the overall system accuracy, intended as "closeness of agreement between a measured quantity value and a true quantity value of a measurand" [33], has been carried out using a 3D aluminum alloy calibrated artifact (see Fig. 7a).

On the artifact, 22 points have been calibrated using a CMM in order to have a set of reference points with known nominal positions. The artifact calibration and the accuracy testing have been carried out by keeping the same, constant environmental conditions (temperature T=21°C; relative humidity RH=27%). The artifact has thus been moved in s=5 different positions, distributed within the measurement volume in order to include worst-case conditions (i.e., volume spatial limits). For each artifact repositioning, the set of reference points have been measured using the MScMS-II. To compare nominal with measured 3D coordinates, the measurement results have been roto-translated using a robust least square (RLS) fitting approach in order to best fit the nominal positions (see Fig. 7b).

Figure 8 shows the histogram of the distances between measured and nominal positions. It is noteworthy how the 50% of the measured points is within a distance of 1.87 mm from the nominal position, while the 94.2% of results is far less than 5 mm from the nominal position. The extent of measurement errors and their high variability are strongly dependent on the severity of experimental testing procedure. As a matter of fact, the results are affected by several issues (e.g., geometric distortion of the reconstructed working volume and measurement process) whose effects on measurement results are different according to the location within the working volume.

According to the results obtained by these experimental tests, the MScMS-II prototype do not provide competitive performance with respect to available commercial systems such as CMMs, laser trackers, iGPS, etc. Those technologies, in the same working volume, are characterized by a measurement uncertainty ranging from few micrometers up to 1 mm at worst, depending on the system, the working conditions, and the measurement procedure [10, 11, 23]. However, these results become particularly interesting if cost and potentiality of the metrological system are considered. Whereas its distributed architecture ensures scalability and flexibility that existing commercial systems cannot guarantee, the prototype still has significant room for enhancement mainly related to the sensing technology. Current CCD sensors (128×96 pixels), although very cheap, significantly affect the metrological performance. An improvement of the network hardware could provide a considerable increase (one order of magnitude at least) in system accuracy, by implementing commercial optical technologies with a limited impact on the cost of the entire system.

6 Conclusions

A low-cost optical IR-based system for indoor coordinate measurement of large-sized objects has been presented and preliminarily characterized through experimental testing.

The system demonstrated to be portable and easy to set up due to its modular architecture and to the exploitation of self-localization procedures for configuring the network independently on the working environment. Rapid measurements are provided by a robust image acquisition and processing system, at frequencies up to 100 Hz. According to its distributed-based architecture, the MScMS-II system is able to extend its measurement capabilities to working environments characterized by large volumes and complex geometries.

The sensor device performance and the overall system capabilities in locating a single point as well as a 3D feature

Table 4 Mean and standard deviation results for reproducibility preliminary tests

	$\bar{x}$ [mm]	$\bar{y}$ [mm]	$\bar{z}$ [mm]	$\hat{\sigma}_X$ [mm]	$\hat{\sigma}_Y$ [mm]	$\hat{\sigma}_Z$ [mm]
Point 1	176.77	333.15	277.87	2.49	1.76	1.54
Point 2	224.39	−70.61	276.91	1.67	0.66	1.21
Point 3	−206.23	−107.96	265.66	2.54	1.03	1.80
Point 4	−258.53	409.44	266.44	3.45	2.10	2.05
Point 5	11.91	141.64	278.28	2.42	0.83	2.43

The sample mean values refer to a user-defined room-aligned reference coordinate system

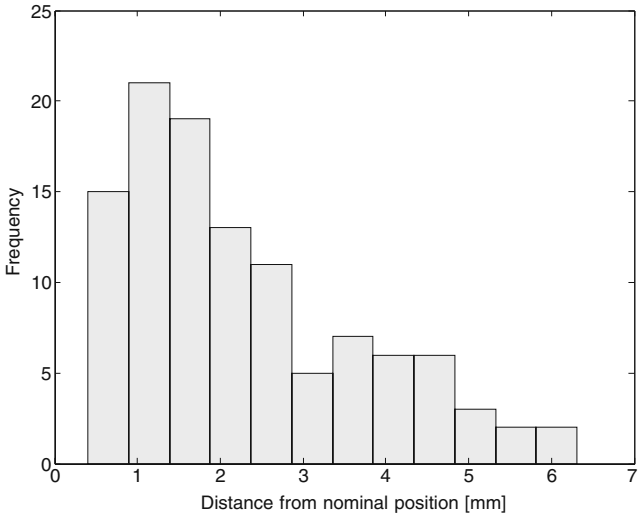

Fig. 8 Accuracy in distance measurement

in a complex working volume have been evaluated. The preliminary results show a great potential of the system for its application in the field of large-scale metrology. Specifically, system metrological characteristics can be improved by increasing the optical sensor resolution and sensitivity, for example, exploiting IR high-resolution cameras. Possible applications of the proposed architecture to metrological systems able to remotely and autonomously move a measuring probe are currently under investigation.

In a research perspective, a closer examination of factors affecting system performance, including IR hardware characteristics, camera synchronization, self-calibration, and localization algorithms, will be carried out. Further investigation should be devoted to the effects of the calibration and scaling procedures and to possible correction models for decreasing the average error. Experimental testing will be used for metrological analysis, uncertainty evaluation as well as for the design of possible correction models, referring to testing procedures used for CMMs. In addition, feasibility of a multi-resolution system, integrating the proposed network-based solution with highly accurate optical systems, will be investigated.

References

1. ARC Second Company (2009) Web site: http://arcsecond.com [Accessed date: 11/02/2009]
2. Automated Precision Inc. (2009) Web site: http://www.apisensor.com/tracker3.html [Accessed date: 04/11/2009]
3. Automated Precision Inc. (2009) Web site: http://www.apisensor.com/intelliprobe.html [Accessed date: 04/11/2009]
4. Axios 3D Services GmbH (2009) Web site http://www.axios3d.de/produkte/messsys/cambar/index_en.html [Accessed date: 04/11/2009]
5. Calibration Matlab tool (2008) Web site: http://cmp.felk.cvut.cz/~svoboda/SelfCal/ [Accessed date: 04/11/2008]
6. Cuypers W, Van Gestel N, Voet A, Kruth J-P, Mingneau J, Bleys P (2009) Optical measurement techniques for mobile and large-scale dimensional metrology. Opt Lasers Eng 47(3–4):292–300
7. Estler WT, Edmundson KL, Peggs GN, Parker DH (2002) Large-scale metrology—an update. Annals of CIRP 51(2):587–609
8. Faro Technologies Inc. (2009) Web site: http://www.faro.com/content.aspx?ct=di&content=pro&item=3 [Accessed date: 16/04/2009]
9. Fischler M, Bolles R (1981) Random sample consensus: a paradigm for model fitting with applications to image analysis and automated cartography. Commun ACM 24(6):381–395
10. Franceschini F, Maisano D, Mastrogiacomo L (2009) Mobile spatial coordinate measuring system (MScMS) and CMMs: a structured comparison. Int J Advanced Manuf Technol 42(11–12):1089–1102
11. Franceschini F, Galetto M, Maisano D, Mastrogiacomo L (2009) Mobile Spatial coordinate Measuring System (MScMS)—introduction to the system. Int J Prod Res 47(14):3867–3889
12. Franceschini F, Galetto M, Maisano D, Mastrogiacomo L (2009) On-line diagnostics in the Mobile Spatial coordinate Measuring System (MScMS). Precis Eng 33:408–417
13. Franceschini F, Galetto M, Maisano D, Mastrogiacomo L (2008) The Problem of Distributed Wireless Sensors Positioning in the Mobile Spatial coordinate Measuring System (MScMS), Proceedings of the 9th ASME Engineering Systems Design and Analysis Conference (ESDA2008), Haifa (Israel), July 07–09
14. Galetto M, Pralio B (2010) Optimal sensor positioning for large scale metrology applications. Precis Eng 34(3):563–577
15. Galetto M, Mastrogiacomo L, Pralio B, Spagnolo C (2010b) Indoor environmental mapping by means of autonomous guided agents, ASME 2010 10th biennial conference on Engineering System Design and Analysis ESDA2010, Istanbul, Turkey, July, 12–14, 2010
16. Hartley RI, Zisserman A (2004) Multiple view geometry in computer vision. Cambridge University Press
17. Hartley RI, Sturm P (1997) Triangulation. J Comput Vis Image Underst 68(2):146–157
18. Hopp TH, Levenson MS (1995) Performance measures for geometric fitting in the NIST algorithm testing and evaluation program for coordinate measurement systems. J Res Natl Inst Stand Technol 100(5):563–574
19. Leica Geosystems (2009) Web site http://metrology.leica-geosystems.com/en/Products-Laser-Tracker-Systems_69045.htm [Accessed date: 04/11/2009]
20. Leica Geosystems (2009) Web site http://metrology.leica-geosystems.com/en/Products-Total-Stations-TPS_4207.htm [Accessed date: 04/11/2009]
21. Longuet-Higgins HC (1981) A computer algorithm for reconstructing a scene from two projections. Nature 293:133–135
22. Luhmann T (2009) Precision potential of photogrammetric 6DOF pose estimation with a single camera. ISPRS J Photogramm Remote Sens 64:275–284
23. Maisano D, Jamshidi J, Franceschini F, Maropoulos PG, Mastrogiacomo L, Mileham AR, Owen GW (2009) Comparison of two distributed large volume measurement systems: MScMS and iGPS. Proceedings of the Institution of Mechanical Engineers. Part B. J Eng Manuf 223(5):511–521
24. Metronor Corporate (2009) web site: http://www.metronor.com [Accessed date: 10/06/2009].
25. Mikhail EM, Bethel JS, McGlone JC (2001) Introduction to modern photogrammetry. Wiley, New York
26. Nikon Metrology (2010) Web site: http://www.nikonmetrology.com/large_volume_tracking__positioning/igps [Accessed date: 25/02/2010]

27. Nikon Metrology (2010) Web site: http://www.nikonmetrology.com/optical_cmm [Accessed date: 25/02/2010]
28. Northern Digital Inc. (2010) Web site http://www.ndigital.com/industrial/products-pcmm.php [Accessed date: 04/11/2009]
29. Peggs GN, Maropoulos PG, Hughes EB, Forbes AB, Robson S, Ziebart M, Muralikrishnan B (2009) Recent developments in large-scale dimensional metrology, Proceedings of the Institution of Mechanical Engineers, Part B. J Eng Manuf 223(6):571–595
30. Puttock MJ (1978) Large-scale metrology. Annals of CIRP 27 (1):351–356
31. Svoboda T, Martinec D, Pajdla T (2005) A convenient multicamera self-calibration for virtual environments. Presence: Teleoperators Virtual Environ 14(4):407–422
32. Tsai RY (1987) A versatile camera calibration technique for high-accuracy 3D machine vision metrology using off-the-shelf cameras and lenses. IEEE J Robot Autom 3(4):323–344
33. VIM—international vocabulary of basic and general terms in metrology (2008) International Organization for Standardization, Geneva, Switzerland
34. Zhang Z (2000) A flexible new technique for camera calibration. IEEE Trans Pattern Anal Mach Intell 22(11):1330–1334